Biosystems Engineering 238 (2024) 38–50

Contents lists available at ScienceDirect

Biosystems Engineering

journal homepage: www.elsevier.com/locate/issn/15375110

Research Paper

Development of a crop growth model for the energy analysis of controlled agriculture environment spaces

Marie-Hélène Talbot *, Danielle Monfet

École de Technologie Supérieure, Montreal, Quebec, Canada

ARTICLE INFO

Keywords:
Controlled environment agriculture
Crop growth
Heat gain/loss from crops
TRNSYS
Energy use

ABSTRACT

In controlled environment agriculture spaces, the conditions fluctuate between photoperiod and dark period, with crops growing continuously. As crops grow, their impact on the energy demand and energy use, often estimated using a building performance simulation tool, becomes more prominent. In this paper, a dynamic crop model integrated into a building performance simulation tool is proposed to estimate the yield and heat gain/loss from crops by combining a growth model and an energy balance model of the crops. The developed growth model is an adjusted version of a greenhouse lettuce growth model modified for high-density controlled environment agriculture applications by calibrating the sensitive parameters for several indoor environment conditions (temperature, lighting, etc.) using an experimental growth dataset. The yield, the energy demand and the energy use were assessed for a case study modelled in TRNSYS. The results obtained using the greenhouse and developed growth models were compared to those generated with the experimental growth dataset. Depending on the indoor environment conditions, the difference in specific energy use estimated using the experimental growth dataset and the developed model varied between 0.1% and 3.5%, indicating that the model led to an acceptable level of accuracy. The dynamic crop model estimates yield and heat gain/loss from crops for various indoor environment conditions, which are essential for carrying out energy, financial, and environmental analyses.

1. Introduction

Controlled environment agriculture (CEA), such as stand-alone agricultural building (greenhouse, plant factory, vertical farm, container farm) or building-integrated agriculture (BIA) (rooftop greenhouse, BIA space with electric and natural lighting), is a promising strategy for year-round crop production. When the crops are stacked vertically, these spaces can be classified as high-density CEA spaces, also known as indoor plant environments without sunlight or vertical farms. These are suitable for local production in cold climates and dense urban areas. High-density CEA spaces enhance crop growth by maintaining specific indoor environmental conditions – temperature, humidity, carbon dioxide (CO_2) concentration, lighting intensity, spectrum, and duration. Protecting the crops from the outdoors while providing optimal growing conditions improves the yield significantly. Still, it also leads to high energy consumption, primarily due to lighting, cooling and dehumidification.

Various indoor environment conditions and novel growing approaches are constantly explored to enhance yield without jeopardising nutritional quality. For example, under high photosynthetically active radiation (PAR) levels and optimal nutrient uptake, the cultivation cycle to obtain 250 g lettuce head can be as low as 18 days (Carotti et al., 2021). However, when searching for the best growing conditions, the impact of the explored conditions on energy consumption is rarely assessed, as the focus is mostly on yield and quality. Consequently, designing and operating CEA spaces that balance yield and energy consumption is challenging. To address those issues, energy modelling can be used to support the analysis of complex thermal processes of CEA operation, such as evaluating different energy-efficient operation strategies (Iddio, Wang, Thomas, McMorrow, & Denzer, 2020). To enhance the energy analysis of CEA spaces by estimating yield and energy consumption, the modelling of a CEA space, often completed using a building performance simulation (BPS) tool, must incorporate the heat exchanges between the crops and their environment, the heat/gain from crops, as the crops grow (El Ghoumari, Tantau, & Serrano, 2005).

A limited number of studies have considered yield and crops as additional internal gain/loss in a BPS tool, and their characteristics, including the different approaches, are compiled in Table 1. Benis, Reinhart, and Ferrão (2017), Graamans, Baeza, van den Dobbelsteen,

* Corresponding author.
E-mail address: marie-helene.talbot.1@ens.etsmtl.ca (M.-H. Talbot).

https://doi.org/10.1016/j.biosystemseng.2023.12.012
Received 18 September 2023; Received in revised form 21 December 2023; Accepted 23 December 2023
Available online 5 January 2024

Nomenclature

Acronyms

BIA	Building-integrated agriculture
BPS	Building performance simulation
CEA	Controlled environment agriculture
CVRMSE	Coefficient of Variation of the Root Mean Square Error
DLI	Daily light integral
HVAC	Heating, ventilation and air conditioning
MAD	Maximum Absolute Difference
LA	Leaf area per plant
LAI	Leaf area index
PAR	Photosynthetically active radiation
PCD	Planting crop density
PPFD	Photosynthetic photon flux density
RMSE	Root mean square error
SHR	Sensible heat ratio
VPD	Vapour pressure deficit

Symbols

CO_2	carbon dioxide
DW	dry weight
FW	fresh weight

Subscripts

leaf	leaf
tot	total
sht	shoot

Tsafaras, and Stanghellini (2018), and Zhang and Kacira (2020) selected a mechanistic growth model to assess yield but calculated the heat gain/loss from crops independently using a fixed leaf area index (LAI) or fixed evaporation rate. The LAI is a dimensionless variable defined as the total one-sided area of photosynthetic tissue per unit of ground surface area (Watson, 1947). Ward, Choudhary, Cundy, Johnson, and McRobie (2015), Jans-Singh, Ward, and Choudhary (2021), and Talbot, Lalonde, Beaulac, Haillot, and Monfet (2022) selected a mechanistic growth model to estimate dynamic heat gain/loss from crops. On the other hand, Talbot and Monfet (2021) Ledesma, Nikolic, and Pons-Valladares (2022), Yeo et al. (2022), and Song, Liu, Pan, Cheng, and Meng (2023) chose an empirical growth model to estimate dynamic heat gain/loss from crops.

Thus, energy analysis completed using a BPS tool must include modelling crop growth and the heat exchanges between crops and their environment. Furthermore, it must also consider the impact of light interception by crops on lighting heat gain. An overview of modelling approaches for each of these phenomena is provided in sections 1.1 to 1.3.

1.1. Modelling the crop growth

Crop growth is influenced by air temperature, light intensity and CO_2 concentration. As crops grow, physiological variables such as root and shoot dry weights, water mass and leaf area change over time. The fluctuation of those variables can be predicted using either empirical or mechanistic models. The different models predict growth from a transplant to a harvest size for lettuces. Empirical models use one or many functions that are developed through data fitting. Those functions are easy to implement, but their application is generally limited. They can be bound to one set of growing conditions or a range of growing conditions. Shimizu et al. (2008) have developed a growth model applicable to lettuces growing at a wide range of CO_2 concentrations (400 and 1200 ppm) and a narrow range of lighting intensities (140–200 μmol $m^{-2}{\cdot}s^{-1}$), but with all of the other conditions being fixed. Hang, Lu, Takagaki, and Mao (2019) have developed a growth model that can use different air temperatures and lighting intensities as inputs, but that was validated over a limited set of conditions, such as low CO_2 concentration. Growth models can also be discretised into sub-models corresponding to a stage of growth (Yeo et al., 2022). On the other hand, mechanistic plant growth models are algorithms that model plant physiological processes such as light interception, photosynthesis rate and respiration loss. They are generally more robust than empirical models. However, in some cases, they use parameters from the literature that do not match the specific growing conditions, potentially leading to "erroneous predictions" (Both, 1995). Many mechanistic models, such as those proposed by Critten (1991), Van Henten (1994), Pearson, Wheeler, Hadley, and Wheldon (1997) and Zhang, Burns, and Turner (2008), are extended versions of the model proposed by Sweeney, Hand, Slack, and Thornley (1981) for which two outputs, the structural dry weight and the non-structural dry weight, are calculated to assess the total dry weight. Another category of mechanistic models is based on a balance of carbon flows, such as the NICOLET model (Seginer, Straten, & Buwalda, 1998) or an adaption to lettuce by Jans-Singh et al. (2021) of a tomato yield model (Vanthoor et al., 2011). More recently, artificial intelligence approaches, such as machine learning (Cohen et al., 2022) and fuzzy logic and neural networks (Chang, Chung, Fu, & Huang, 2021), have also been used to predict crop growth.

Three of the studies in Table 1 selected the mechanistic growth model proposed and validated by Van Henten (1994) to model lettuce growth in a CEA space. This model is based on principles from plant physiology and parameters selected from the literature. It estimates the total dry weight (structural and non-structural) of lettuces (*Lactuca sativa* L.) as a function of air temperature, solar irradiance and CO_2 concentration. The model was validated experimentally for two cultivars in a semi-controlled greenhouse, and the indoor conditions were monitored for 56 days. Over this period, the air temperature varied between 7 °C and 24 °C (mean value of 12 °C), the mean daily light integral (DLI), which is the number of photosynthetically active photons delivered to a specific area over 24 h, was 5 $mol{\cdot}m^{-2}{\cdot}d^{-1}$ and the CO_2 concentration varied between 347 ppm and 776 ppm (mean value of 464 ppm). In high-density CEA spaces, air temperature, DLI and CO_2 concentration are maintained at a higher level than the one used to validate the model. Thus, it is unclear if this model suits high-density CEA applications. Graamans et al. (2018) commented that the model might underestimate dry matter production for higher temperatures, which are usually maintained in those spaces compared to a semi-controlled greenhouse.

1.2. Modelling heat gain/loss from crops

Different approaches have been proposed to model heat gain/loss from crops, i.e., the latent heat gain and the sensible heat gain/loss, in BPS tools. These include using a fixed evaporation rate, fixed LAI or a dynamic LAI, as reported in Table 2.

Using a fixed stage of growth is appropriate for sizing the heating, ventilation and air conditioning (HVAC) equipment or for modelling crops that are growing according to a diversified stage growth management method (Talbot & Monfet, 2020). Still, it is not sufficiently precise to establish the energy use as the crops grow.

1.3. Modelling light interception

Modelling light interception has two functions: (1) determining the useful fraction of the PAR emitted by lights absorbed by crops, which influences both the heat gain/loss from crops and growth and (2)

Table 1
Characteristics of studies that incorporated crops as an additional internal gain/loss in a BPS tool and growth model to model a CEA space.

Reference	BPS tool	Space Type[1]	Crop Type	Type of growth model	Dynamic heat gain/loss from crops
Ward et al. (2015)	TRNSYS	RTGH	Tomato	Mechanistic model (Vanthoor, de Visser, Stanghellini, van Henten, 2011)	☑
Benis et al. (2017)	EnergyPlus	RTGH BELO BENL	Tomato	Mechanistic model (Vanthoor, de Visser, Stanghellini, & van Henten, 2011)	
Graamans et al. (2018)	EnergyPlus	GH PF	Tomato	Mechanistic model (Van Henten, 1994)	
Zhang and Kacira (2020)	EnergyPlus	PF	Lettuce	Mechanistic model (Van Henten, 1994)	
Talbot and Monfet (2021)	TRNSYS	BELO	Lettuce	Empirical model (Shimizu, Kushida, & Fujinuma, 2008)	☑
Jans-Singh et al. (2021)	EnergyPlus	BENL	Lettuce	Mechanistic model (adaptation of Vanthoor et al. (2011) to lettuce)	☑
Ledesma et al. (2022)	EnergyPlus	RTGH	Lettuce	Empirical model based on data from Fraile-Robayo, Álvarez-Herrera, Reyes M, Álvarez-Herrera, Fraile-Robayo (2017)	☑
Talbot et al. (2022)	TRNSYS	CF	Lettuce	Mechanistic model (Van Henten, 1994)	☑
Yeo et al. (2022)	TRNSYS	RTGH	Tomato	Empirical model discretised in seven stages of growth	☑
Song et al. (2023)	EnergyPlus	CF	Lettuce	Empirical model	☑

[1] Stand-alone spaces | PF: Plant factory, CF: Container farm, GH: Stand-alone greenhouse.
[1] Building integrated agriculture (BIA) spaces | BELO: BIA space with electric lighting only, BENL: BIA space with electric.
[1] and natural lighting, RTGH: Rooftop greenhouse.

determining the lighting heat gain. A few studies incorporated the impact of light interception on lighting heat gain (Kokogiannakis & Cooper, 2015; Liebman-Pelaez, Kongoletos, Norford, & Reinhart, 2021; Talbot & Monfet, 2020), and one incorporated it as a dynamic variable that varies with growth (Talbot & Monfet, 2021). Light interception is a thermal phenomenon that cannot be neglected to comply with the law of energy conservation.

The previous sections have highlighted the different approaches used to model crops and how they were integrated into BPS tools. The proposed approaches to model growth and heat gain/loss from crops lack integration, suitability to CEA applications and versatility across several indoor conditions. In this paper, a dynamic crop model that can predict the growth and heat gain/loss from crops for several indoor environment conditions, integrated into a BPS tool, is proposed. It is a grey-box model parametrised using an experimental growth dataset from the literature that predicts yield and heat gain/loss from crops for several

Table 2
Approaches to estimate heat gain/loss from crops in BPS tools.

Approach	Reference
1) Fixed evaporation rate	Harbick and Albright (2016) Zhang and Kacira (2020)
2) Fixed leaf area index	Kokogiannakis and Cooper (2015) Benis et al. (2017) Nadal et al. (2017) Graamans et al. (2018) Lalonde, Talbot, and Monfet (2019) Baglivo et al. (2020)
3) Dynamic leaf area index that varies according to growing conditions in a transient modelling approach	Ward et al. (2015) Jans-Singh et al. (2021) Talbot and Monfet (2021) Ledesma et al. (2022) Talbot et al. (2022) Yeo et al. (2022) Song et al. (2023)

indoor environment conditions. It is intended to be part of a versatile and transient approach developed in the TRNSYS software (Klein and al, 2017) that aims to improve CEA space energy, financial and environmental analyses. This study focuses on developing a lettuce model because it is one of CEA's most commonly cultivated species (Agritecture & WayBeyond, 2021) and can be grown in vertical stacks.

2. Methods

This section presents the developed model, its parametrisation and calibration using an experimental growth dataset available in the literature, and its implementation for energy analysis. The implementation is verified by comparing the use of the experimental growth dataset versus the outputs of the dynamic crop model to estimate the yield, the energy demand, and the energy use over a cultivation cycle combined into two indicators: the specific energy demand for lighting, cooling, dehumidification and heating as well as the specific energy use. These are estimated by dividing the maximum energy demand per category and the energy used by the shoot fresh weight harvested over one cultivation cycle. The energy demand includes the electric energy demand for lighting as well as the rate of energy that the space requires to maintain the indoor environment at desired conditions for cooling, dehumidification, and heating. In this context, the energy use is the integral of the energy demand (lighting, cooling, dehumidification and heating) over one cultivation cycle. The energy demand is influenced by the heat gains/losses from external sources (conduction through building envelope, solar heat gain through fenestration, ventilation and infiltration) and internal sources (occupants, lighting, equipment and crops). As such, the energy demand does not include the impact of any HVAC equipment, such as the sensible heat gain of a dehumidifier located in the space or the latent heat removal associated with the sensible cooling process or the efficiency of the equipment.

2.1. Dynamic crop model

The dynamic crop model developed in this study combines two sub-models, the growth model and the energy balance model, with intermediary variables being exchanged between the two sub-models (Fig. 1). The growth model estimates, at every timestep, the total (shoot and root) plant dry weight (DW_{tot}). The shoot fresh weight (FW_{sht}) and the LAI are estimated using the total plant dry weight. The shoot fresh weight is used to estimate yield, while the LAI is used to estimate the heat gain/loss from crops and the PAR not absorbed by crops, two variables transferred to the thermal zone model. The heat gain/loss from crops are incorporated as additional internal gains/losses at the airnode energy balance solved according to the heat balance method, while the

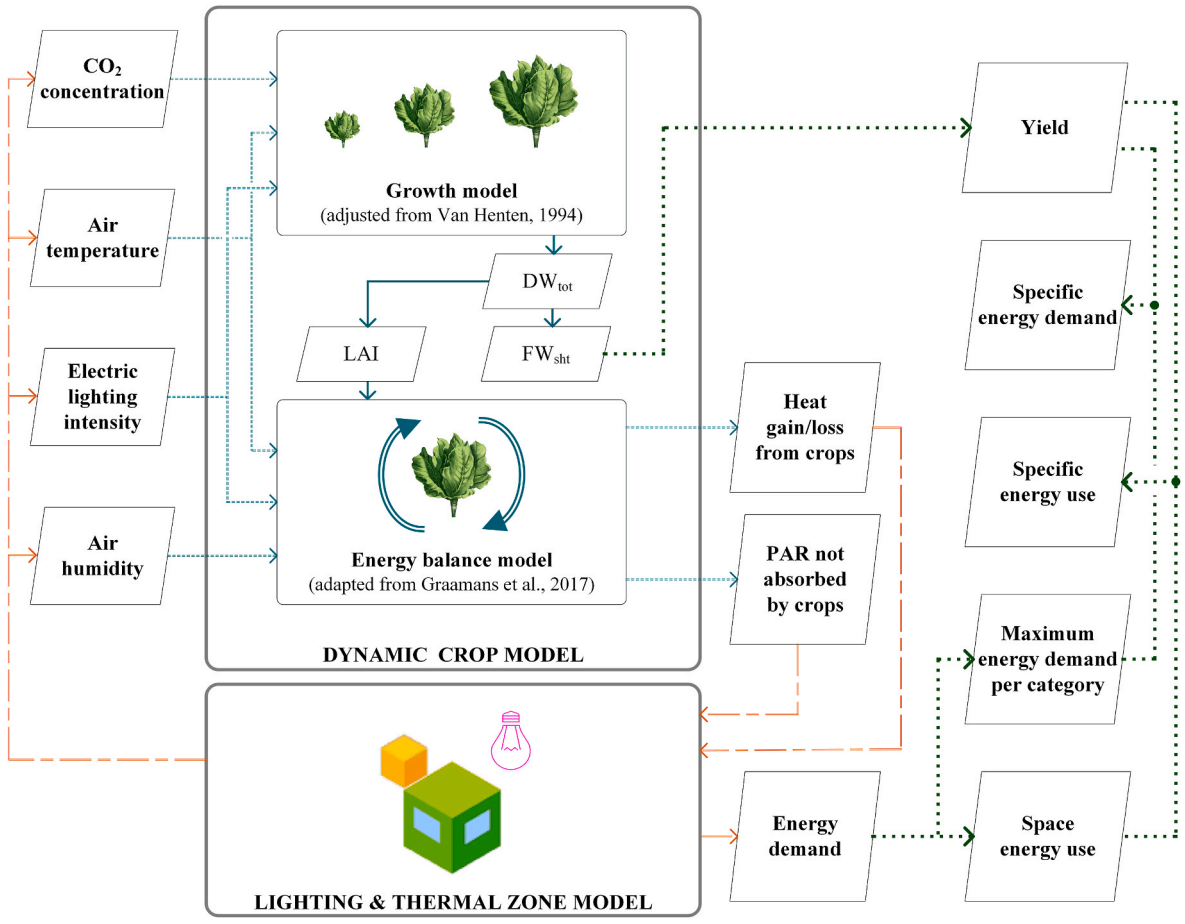

Fig. 1. Overview of the dynamic crop model developed as a TRNSYS component.

PAR not absorbed by crops is used to estimate the lighting heat gain.

2.1.1. Growth model

The adjusted growth model is an adaptation of the algorithm proposed by Van Henten (1994) coded according to the equations and parameters summarised in Supplementary Tables A1 and A2. This model was developed to be used solely with solar PAR. Thus, it is first modified, as expressed by Equation (1), to account for both PAR sources (solar and electric lighting) to make it suitable for CEA applications.

$$PAR = c_{sol_{to}PAR} \bullet q''_{sol} + c_{PPFD_{to}PAR} \bullet PPFD \quad (1)$$

where *PAR* is the total photosynthetic active radiation that includes both solar and electric lighting ($W \cdot m^{-2}_{cultivated}$); $c_{PPFD_{to}PAR}$ is the fraction of the total solar spectrum that is PAR, set to a value of 0.44; $c_{PPFD_{to}PAR}$ is the conversion factor from PPFD to the equivalent solar PAR, set to a value of 0.217 $W \cdot m^{-2}_{cultivated} \cdot (\mu mol \cdot m^{-2} \cdot s^{-1})^{-1}$ (Dorais, 2003); and *PPFD* is the photosynthetic photon flux density from electric lighting ($\mu mol \cdot m^{-2} \cdot s^{-1}$).

The growth model is then parametrised by (1) modifying some parameters according to recent literature or to be more suitable to high-density CEA applications and (2) calibrating the parameters of the growth model that were previously identified as sensitive (Van Henten & Van Straten, 1994) using an experimental growth dataset from Carotti et al. (2021) detailed in Table 3. Carotti et al. reported the shoot fresh weight (FW_{sht}) and total dry weight (DW_{tot}) per plant for lettuce (*Lactuca sativa cv. Batavia Othilie*) growing in a CEA space under different PPFD and indoor air conditions with a planting crop density of 25 plant•m^{-2}. Those conditions were reported for a root temperature of 28 °C, a vapour pressure deficit (VPD) that alternated between 0.58 kPa and 0.34 kPa for the photoperiod and dark period, respectively, a CO_2 concentration of 1200 ppm and a photoperiod of 16 h. The growth model is calibrated from a transplant weight of 1.2 g_{FW}•$plant^{-1}$ with a dry matter content estimated to be 5% (Puccinelli, Malorgio, Pintimalli, Rosellini, & Pezzarossa, 2022) to the moment the shoot fresh weight reaches a marketable weight of 250 g_{FW}•$plant^{-1}$.

Four sensitive parameters (Van Henten & Van Straten, 1994), light use efficiency at very high CO_2 concentration (c_ε), yield factor (c_β),

Table 3
Experimental growth dataset used to parametrise the growth model (Carotti et al., 2021).

Conditions	Low PPFD			Medium PPFD			High PPFD		
PPFD, $\mu mol \bullet m^{-2} \bullet s^{-1}$	200			400			750		
DLI, $mol \bullet m^{-2} \bullet d^{-1}$	11.5			23.0			43.0		
$DW_{content}$ at harvest, %	2.6			3.8			4.2		
Air temperature, °C	20	24	28	20	24	28	20	24	28
Relative humidity (photoperiod/dark period), %	75/85	80/89	85/91	75/85	80/89	85/91	75/85	80/89	85/91
SLA, $cm^2 \cdot g^{-1}_{DW}$	360	436	400	295	300	314	244	272	250
Cultivation cycle, days	28.0	25.3	27.0	21.2	19.0	23.6	18.3	18.1	21.2

extinction coefficient (k_s) and saturation growth rate ($c_{gr,max}$), are calibrated using the growth experimental dataset. Calibration is used to match the output of a model with measured data by modifying its parameters. There is no consensus on the approach or criteria to use for the calibration of growth models. López-Cruz, Ruiz-García, Fitz-Rodríguez, Salazar-Moreno, and Rojano-Aguilar (2017) compared three calibration methods, a classic nonlinear least squares method and two Bayesian methods, to improve the prediction of lettuce dry weight with a growth model. Different criteria were used depending on the method, such as the sum of the square error and the root mean square error (RMSE). They concluded that the methods all performed similarly. Two techniques were employed sequentially by Ramirez, Rodriguez, Berenguel, and Heuvelink (2003) to calibrate a tomato growth model: least squares identification methods and a genetic algorithm. Due to the limited availability of information on the subject, it may be advisable to employ best practices for calibrating BPS models, as the developed growth model is integrated into this type of tool. The calibration of BPS models, specifically building energy models, can be automated or manual, depending on the number of parameters to calibrate. Automated calibration is characterised by programmed mathematical procedures or analytical approaches to complete the calibration procedure (Coakley, Raftery, & Keane, 2014), such as statistical methods (e.g., Bayesian approach) and evolutionary algorithms (e.g., genetic algorithm). Baba, Ge, Zmeureanu, and Wang (2022) reported that Bayesian approaches have been used to calibrate unknown input variables, while genetic algorithms have been used in several studies for the auto-calibration of energy consumption. They also concluded that genetic algorithms required fewer simulations to obtain a calibrated model. Thus, the variables c_ε, c_β, k_s, $c_{gr,max}$ are calibrated using a genetic algorithm that minimises the RMSE between the shoot fresh weight estimated with the growth model and the shoot fresh weight reported by Carotti et al. (2021). The shoot fresh weight estimated with the growth model is calculated according to equation (2) based on the total dry weight from the growth model. The parameters' bounds are listed in Table 4, and the genetic algorithm is limited to a maximum of 200 generations and a population size of 50.

$$FW_{sht}(t) = DW_{sht}(t) \,/\, DW_{content} = [(1 - c_\tau) \bullet DW_{tot}(t)] \,/\, DW_{content} \tag{2}$$

where FW_{sht} is the shoot fresh weight (g_{FW}•$plant^{-1}$); $DW_{content}$ is the dry matter content (g_{DW}·g_{FW}^{-1}); DW_{sht} is the shoot dry weight (g_{DW}•$plant^{-1}$); DW_{tot} is the total dry weight (g_{DW}•$plant^{-1}$); and c_τ is the ratio of the root dry weight to the total dry weight.

Statistical criteria, such as the Coefficient of Variation of the Root Mean Square Error (CVRMSE) and the Maximum Absolute Difference (MAD), are also calculated, as proposed by Baba et al. (2022), to compare the obtained results.

2.1.2. Energy balance model

The energy balance model adapts the algorithm proposed by Graamans, van den Dobbelsteen, Meinen, and Stanghellini (2017). The energy balance is defined by equation (3), where the latent and sensible gain/loss from crops are defined by equations (4) and (5) and the net radiation terms by equations (7) and (8), and where the thermal storage in the leaf and stems is considered negligible (Stanghellini, 1987). Every term of the energy balance equation varies with leaf growth, which is considered using the LAI. The LAI, as defined by equation (6), is proportional to the leaf area per crop (LA) and the planting crop density (PCD), (Kozai, 2016). The system of equations is solved using the modified secant method, which has been adapted to calculate moist air properties dynamically.

$$q'_{plt,sol} + q'_{plt,SW} - q'_{plt,conv} - q'_{plt,latent} = 0 \tag{3}$$

$$q'_{plt,latent} = LAI \bullet \lambda \frac{\chi_s - \chi_a}{r_s + r_a} \tag{4}$$

$$q'_{plt,conv} = LAI \bullet \rho_{a,i} \bullet c_{p_{a,i}} \frac{T_{plt} - T_{a,i}}{r_a} \tag{5}$$

$$LAI = PCD \bullet LA \tag{6}$$

where the net radiation flux absorbed by the crops can be from solar radiation ($q'_{plt,sol}$) and/or the short-wave radiation from electric lighting ($q'_{plt,SW}$) (W·$m^{-2}_{cultivated}$); $q'_{plt,latent}$ is the latent heat flux from crops (W·$m^{-2}_{cultivated}$); $q'_{plt,conv}$ is the convective heat flux (gain or loss) from crops (W·$m^{-2}_{cultivated}$); LAI is the Leaf Area Index (m^2_{leaves}·$m^{-2}_{cultivated}$); λ is the heat of vaporisation of water (kJ·kg^{-1}); χ_s is the vapour concentration at the canopy level (g·m^{-3}); χ_a is the air vapour concentration (g·m^{-3}); r_s is the stomatal resistance (s·m^{-1}); r_a is the aerodynamic resistance (s·m^{-1}); $\rho_{a,i}$ is the indoor air density (kg·m^{-3});' $c_{p_{a,i}}$ is the specific heat of the indoor air (J·(kg•°C)$^{-1}$); T_{plt} is the leaves temperature (°C); $T_{a,i}$ is the indoor air temperature (°C); LA is the leaf area per plant (m^2_{leaves}·$plant^{-1}$); and PCD is the planting crop density (plant·$m^{-2}_{cultivated}$).

The absorbed PAR ($q'_{sol,plt}$ and $q'_{SW,plt}$), often referred to as net radiation, is the primary input flux to the energy balance of the crops (equation (3)) and represents a portion of the transmitted solar radiation (equation (7)) or PAR emitted by lights (equation (8)) depending on the light interception. The light interception fraction (i.e., $1 - e^{-k_s \bullet LAI}$) is assessed using extinction coefficients as proposed by Katsoulas & Stanghellini, 2019 since it can be applied to various planting crop densities.

$$q'_{plt,sol} = \left(1 - e^{-k_{s,sol} LAI}\right) \bullet q''_{sol} \tag{7}$$

$$q'_{plt,SW} = \left(1 - e^{-k_{s,el} LAI}\right) \bullet q''_{el,SW} \tag{8}$$

where $k_{s,sol}$ and $k_{s,el}$ are the extinction coefficients associated with solar radiation and PAR from electric lighting; q''_{sol} is the transmitted solar radiation flux (W·$m^{-2}_{cultivated}$); and $q''_{el,SW}$ is the short-wave radiation flux from electric lighting (W·$m^{-2}_{cultivated}$).

2.1.3. Light interception modelling

The electric lighting power input (q''_{el}) splits in three: the convective heat gain ($q'_{el,conv}$), the long-wave radiation heat gain ($q'_{el,LW}$), and the short-wave radiation ($q'_{el,SW}$), often referred to as the photosynthetic active radiation (PAR). The energy distribution depends on the lighting heat fractions (convective (f_{conv})/radiative long-wave (f_{LW})/radiative short-wave (f_{SW})) which are specific to the lights model. Only a fraction of the short-wave radiation is intercepted and absorbed by crops ($q'_{plt,SW}$), while the rest is contributing to the lighting heat gain ($q'_{zone,SW}$) as illustrated in Fig. 2. As the leaf coverage over the cultivated area expands, the light interception increases, thereby increasing the radiation absorbed by crops and decreasing lighting heat gain. Light interception is influenced by factors such as cultivated crops, planting crop density and light source.

Table 4
Bounds used for the calibration of the growth model sensible parameters.

Parameter	Lower bound	Upper bound	Reference
c_ε, g·J^{-1}	3•10^{-6}	17•10^{-6}	Set heuristically
c_β	0.4	0.9	López-Cruz et al. (2017)
k_s	0.66	0.9	Tei, Scaife, and Aikman (1996) and Van Henten (1994)
$c_{gr,max}$, s^{-1}	0.5·10^{-6}	5.0·10^{-6}	Set heuristically

2.2. Space model

The modelled space is a 3.02 m × 2.44 m x 1.97 m room located in a

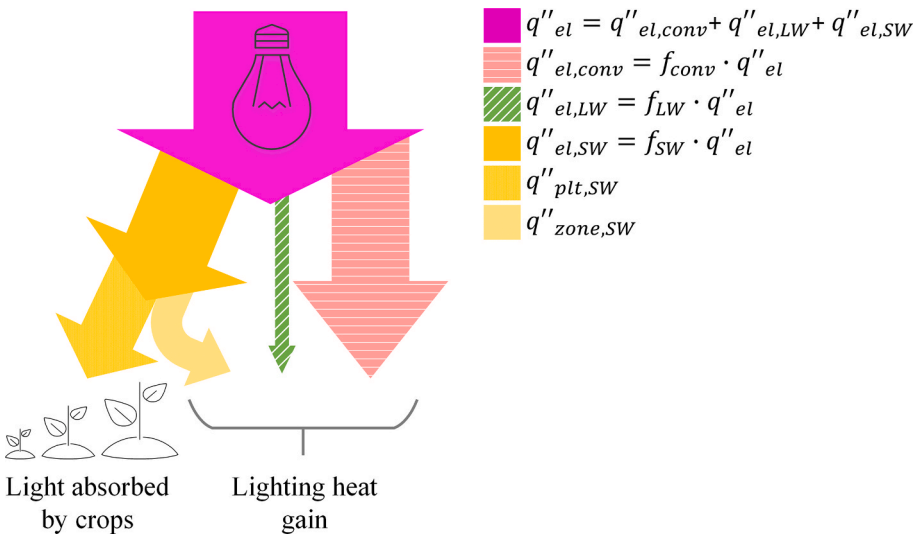

Fig. 2. Energy distribution of the electric lighting power input.

building maintained at an ambient temperature of 20 °C, and the simulation timestep is 10 min. A vertical hydroponic stacking system with a 2.8 m^2 footprint and three tiers with 46.5 cm vertical spacing is installed in the space, as illustrated in Fig. 3. The walls, floor and ceiling have an overall U-value of 0.12 $W{\cdot}(K{\cdot}m^2)^{-1}$, a thermal capacity of 1000 $J{\cdot}(kg{\cdot}K)^{-1}$, and a density of 113.17 kg m^{-3}. They are covered with water-repellent panels to minimise the migration of water vapour through the surfaces. The space is enriched in CO_2 to enhance crop growth and is airtight to avoid the dilution of the CO_2. Moreover, it is assumed that the air is well-mixed and air velocity over the leaves is sufficient to facilitate gas exchange. Indoor conditions alternate between two states: (1) photosynthesis state that occurs during the photoperiod (when the lights are on) and (2) respiration state that occurs during the dark period (when the lights are off). The three tiers are lit with electric lighting, and their heat fractions are assumed to be 0.52/0.11/0.37 ($f_{SW}/f_{LW}/f_{conv}$) as illustrated in Fig. 2.

2.3. Modelling verification

Two different verifications are proposed to ensure the crop model is implemented correctly. First, the reliability of the growth model to predict yields for other lighting intensities that are not part of the experimental growth dataset, specifically at 300 and 500 µmol $m^{-2}{\bullet}s^{-1}$. It is completed by assessing yields at 200, 300, 400 and 500 µmol $m^{-2}{\bullet}s^{-1}$ and the anticipated result is a linear rise in annual yield between 200 and 500 µmol $m^{-2}{\bullet}s^{-1}$ as previously established by Jin, Fomiga Lopez, Heuvelink, and Marcelis (2023). For lighting intensities of 300 and 500 µmol $m^{-2}{\bullet}s^{-1}$, the values of the sensible parameters are determined through interpolation, drawing upon the calibrated values.

Second, to ensure the implementation of the energy balance is accurate, the proposed energy modelling approach is then verified by comparing the estimated energy use per category with those reported by Graamans et al. (2018). This verification is solely for implementing the energy balance model, as the results are for a fixed LAI of 2.1 with a light

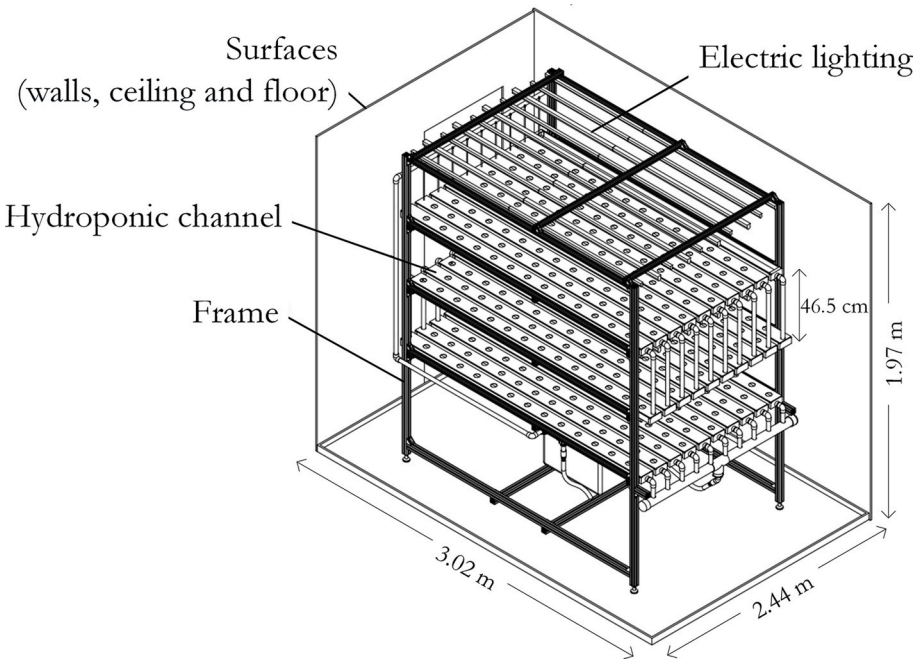

Fig. 3. Small-scale high-density CEA space.

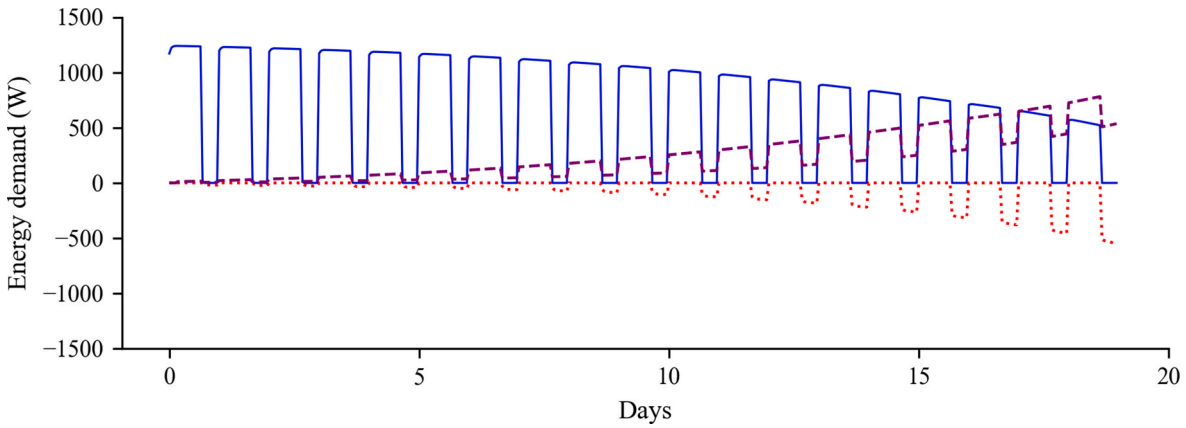

Fig. 4. Energy demand at Medium PPFD @24 °C over a cultivation cycle for cooling (solid line), heating (dotted line) and dehumidification (dashed line) using the experimental growth dataset.

interception fraction of 0.81. The indoor environment conditions are adjusted to match those reported in Table 5, with a planting crop density of 17.6 plant•m^{-2}. Additionally, the cultivated area is increased to 10.2 m^2 to maintain the same ratio of cultivated area over the volume specified in Graamans et al. (2018). For this verification, two alterations are also introduced to the proposed energy modelling approach: (1) the impact of light interception on lighting heat gain is neglected, and (2) moisture removal associated with the sensible cooling process, with a sensible heat ratio of 0.7, is added. The latest is included because the software DesignBuilder accounts for moisture removal when computing the cooling energy demand of the space. The comparison is completed for the energy use by category for lighting, cooling and dehumidification, as detailed in section 3.4.

3. Results

The results are presented for the case study, the small-scale CEA-HD space, for two versions of the developed crop model: (1) with the initial growth model (section 3.2) and (2) with the adjusted growth model (section 3.3) following the proposed modifications and calibration of the most sensitive parameters using a genetic algorithm. Before these results, the approach undertaken to establish the heat gain/loss from crops using the experimental growth dataset (Table 3) is detailed (section 3.1). The results from the verification of the models are presented in section 3.4.

3.1. Heat gain/loss from crops using the experimental growth dataset

The procedure used to assess the specific demand and the specific energy use based on the heat/gain loss from crops using the experimental growth data set is similar to the one illustrated in Fig. 1. However, instead of modelling growth, the growth dataset is used. The dataset by Carotti et al. (2021) reported the shoot fresh weight (FW_{sht}) and total dry weight (DW_{tot}) per plant for lettuce as well as the Specific Leaf Area (SLA) and the dry matter content ($DW_{content}$) instead of the LAI. Thus, the LAI is estimated using the measured shoot fresh weight and dry matter content according to Equations (9) and (10). Equation (9) estimates the LAI based on the planting crop density, the SLA and the leaf dry weight (DW_{leaf}). Equation (10) estimates the leaf dry weight based on the leaves to shoot dry weight ratio (DW_{leaf}/DW_{sht}), the shoot fresh weight and the dry matter content.

$$LAI = PCD \bullet LA = PCD \bullet \left[SLA \bullet DW_{leaf}\right] \tag{9}$$

$$DW_{leaf} = \frac{DW_{leaf}}{DW_{sht}} \bullet DW_{sht} = \frac{DW_{leaf}}{DW_{sht}} \bullet FW_{sht} \bullet DW_{content} \tag{10}$$

Where SLA is the Specific Leaf area (m^2•g$_{DW}^{-1}$); DW_{leaf} is the dry leaf weight (g$_{DW}$•m$_{cultivated}^{-2}$); and DW_{leaf}/DW_{sht} is the leaves to shoot dry weight ratio. It was estimated heuristically based on Carotti et al. (2021) to a value of 0.92.

As an example, the impact of the crops growing on the energy demand for cooling, heating and dehumidification at Medium PPFD/24 °C is illustrated in Fig. 4. As crops grow, the cooling energy demand decreases while the dehumidification energy demand increases during the photoperiods. During the dark periods, additional heating and dehumidification are required towards the end of the cultivation cycle, while the cooling energy demand remains minimal.

3.2. Performance of the initial growth model

The specific energy demand for lighting, cooling, dehumidification and heating and the specific energy use are presented in Figs. 5 and 6 when yield and heat gain/loss from crops are estimated using the experimental growth dataset reported by Carotti et al. (2021) versus the initial growth model. The two indicators are estimated over a cultivation cycle, i.e., from a transplant weight of 1.2 g$_{FW}$•plant^{-1} to a marketable weight of 250 g$_{FW}$•plant^{-1}. The LAI and cultivation cycle calculated using the experimental growth dataset versus the initial growth model are presented in Fig. 7.

As expected, the lighting specific energy demand is not influenced by crop growth while the cooling specific energy demand is slightly influenced by crop growth due to light interception. On the other hand, the dehumidification demand and heating demand depend on the heat gain/loss from crops, which increase as the crops grow. The initial growth model overestimates the specific energy demand for dehumidification and heating, which can be attributed to an overestimation of the LAI, as illustrated in Fig. 7.

The specific energy use is underestimated for most conditions when the initial growth model is used, with a maximum difference of 22.0% (High PPFD@28 °C). This is explained by the shorter cultivation cycle estimated with the initial growth model. However, for some conditions, this is offset by overestimated energy demand for dehumidification and heating, leading to low differences in the specific energy use.

Table 5
Indoor environment conditions of the CEA modelled by Graamans et al. (2018).

Indoor environment conditions	Values
PPFD, µmol•m^{-2}•s^{-1}	500
DLI, mol•m^{-2}•d^{-1}	28.8
Heating setpoint (photoperiod/dark period), °C	24/24
Cooling setpoint (photoperiod/dark period), °C	30/30
Minimum relative humidity (photoperiod/dark period), %	65/65
Maximum relative humidity (photoperiod/dark period), %	90/90

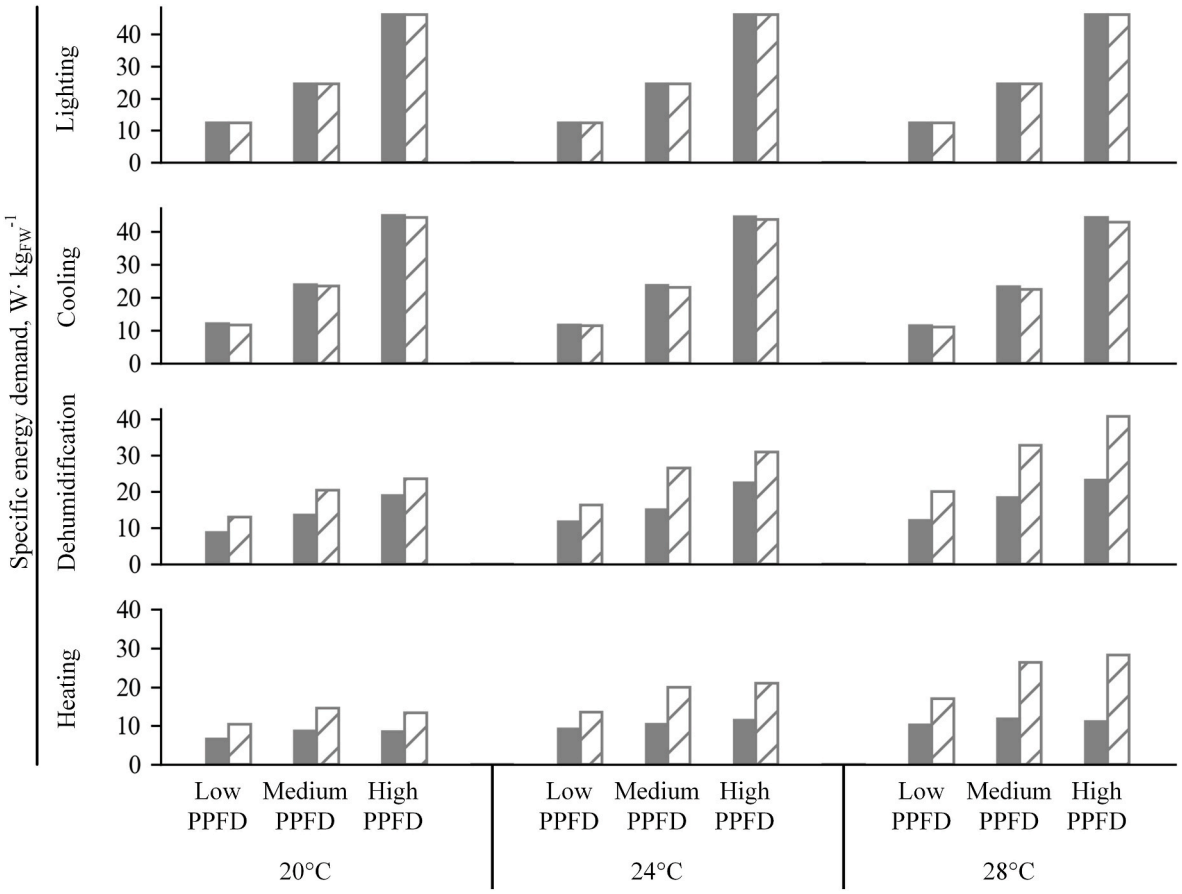

Fig. 5. Specific energy demand estimated using the experimental growth dataset from Carotti et al. (2021) (solid bars) and the initial growth model from Van Henten (1994) (hatched bars) over one cultivation cycle.

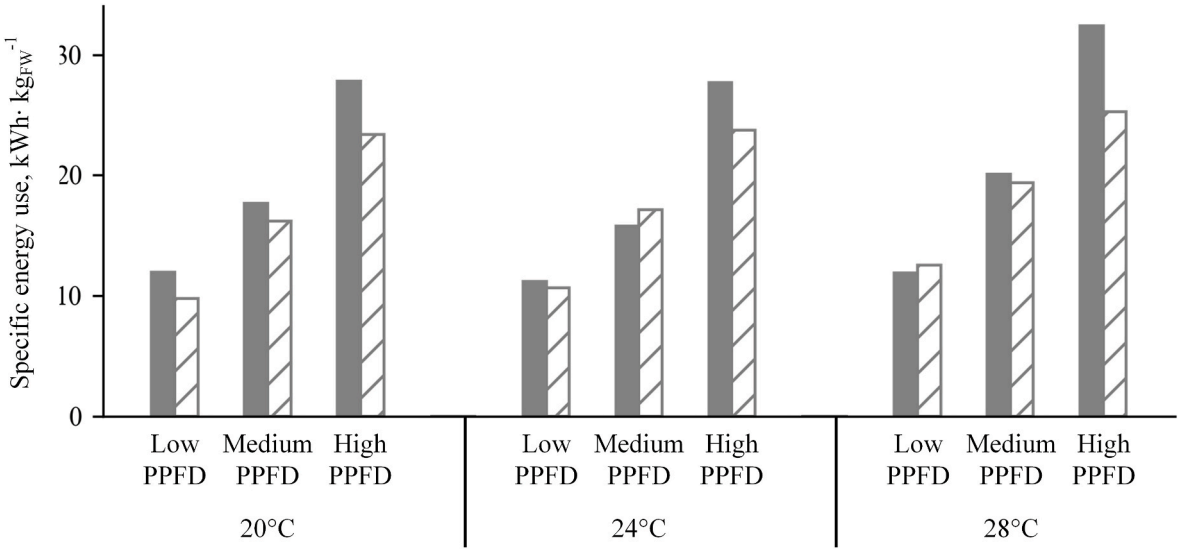

Fig. 6. Specific energy use estimated using the experimental growth dataset from Carotti et al. (2021) (solid bars) and the initial growth model from Van Henten (1994) (hatched bars) over one cultivation cycle.

As illustrated in Fig. 7, the initial growth model overestimates the growth rate for all the conditions, leading to an overly short cultivation cycle. The predicted cultivation cycle is consistently shortened by 2.2% (Medium PPFD@24 °C) to 28.2% (High PPFD@28 °C). The estimation of the maximum LAI is also overestimated by the initial growth model from 51% (Low PPFD@24 °C) to 142% (High PPFD@28 °C).

The results showed that the initial growth model did not perform well in a high-density CEA application. It overestimates the LAI and the growth rate. As a result, it significantly overestimates the specific energy demand for dehumidification and heating and the annual yield. The influence on specific energy use is lessened but underestimated for most conditions. Thus, the model needs to be adjusted to better estimate the

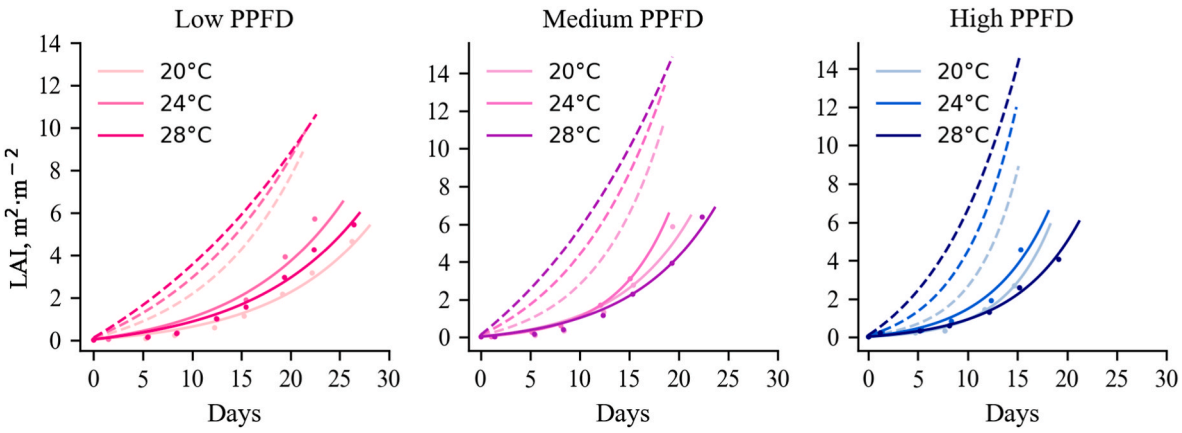

Fig. 7. LAI estimated using the experimental dataset from Carotti et al. (2021) (solid lines including experimental points) and the initial growth model from Van Henten (1994 (dashed lines) over one cultivation cycle.

specific energy demand for dehumidification and heating and the specific energy use of a high-density CEA space.

3.3. Performance of the adjusted growth model

To improve the model, some parameters are modified according to recent literature or to be more suitable to high-density CEA application as listed in the last column of Supplementary Table A2. The boundary conductance (g_{bnd}) and stomatal conductance (g_{stm}) are modified (Table A2) according to Graamans et al. (2017). Additionally, as highlighted in section 3.2 and illustrated in Fig. 7, the LAI estimated using the initial growth model showed substantial differences compared to values derived from the experimental growth dataset. As such, the equation that calculates the LAI (Equation (A.6i)) is modified to Equation (A.6m) to use the specific leaf area (SLA) instead of the structural leaf ratio (c_{lar}) since the SLA is available in recent literature (e.g., Carotti et al. (2021)).

The calibration of the most sensitive parameters of the modified growth model leads to the parametrisation of the growth model shown in Fig. 8, with the corresponding statistical criteria tabulated in Table 6.

The relative differences between the results obtained with the initial and adjusted growth model, compared to the results derived from the experimental growth dataset (Carotti et al., 2021), are presented in Table 7. The differences are reduced to less than 5.2% and 10.4% for the specific energy demand for dehumidification and heating and to 3.5 % for the specific energy use, compared to differences that ranged up to 79.4% and 153.5% for the specific energy demand for dehumidification and heating and 22.0% for the specific energy use with the initial growth model. The difference is reduced to less than 3.5% compared to differences that ranged up to 28.2%.

3.4. Verification of the modelling approach

The results obtained with the adjusted growth model provide additional insight into establishing the energy performance of high-density CEA spaces. The results of two different verifications are presented. First, the ability of the growth model to predict yields for lighting intensities that were not included in the experimental growth dataset described in Table 3 is completed. The estimated yields for 200, 300, 400 and 500 µmol m^{-2}•s^{-1} are depicted in Fig. 9. As expected, the figure illustrates linear correlations between predicted yield and lighting intensity. The R-square values obtained range from 0.8645 to 0.9201, demonstrating a satisfactory level of robustness of the model.

Second, to ensure that the implementation of the energy balance is accurate, a comparison of the estimated energy use by category with those reported by Graamans et al. (2018) is completed. As such, the model and the energy modelling approach are altered according to the information listed in section 2.3. As previously stated, this is solely for implementing the energy balance model as the results are for a fixed LAI of 2.1, a light interception fraction of 0.81 without considering its impact on the zone heat gain, crop density of 17.6 plant•m^{-2}, cultivated area of 10.2 m^2, PPFD of 500 µmol m^{-2}•s^{-1}, DLI of 28.8 mol m^{-2}•d^{-1}, temperature between 24 and 30 °C, relative humidity between 65 and 90%, and a sensible heat ratio of 0.7. The comparison is completed over the lighting, cooling and dehumidification energy use intensity, as illustrated in Fig. 10. Upon altering the proposed modelling approach, which only applies to the results presented in Fig. 10, it is observed that the discrepancies for the cooling and dehumidification are 5% and 1%,

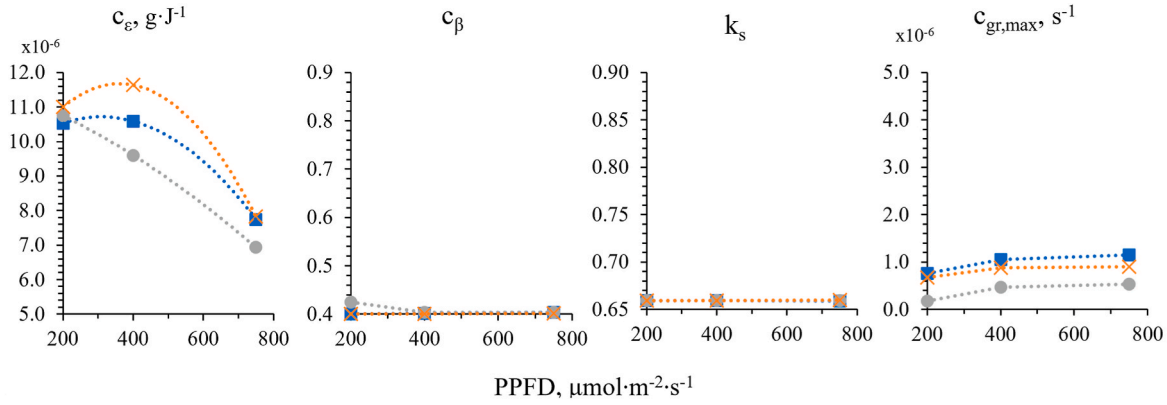

Fig. 8. Calibrated sensible parameters for ■ 20 °C, × 24 °C, and ● 28 °C.

Table 6
Statistical criteria of the calibration minimising the RMSE of the fresh weight per plant.

	Low PPFD (200 µmol m^{-2}•s^{-1})			Medium PPFD (400 µmol m^{-2}•s^{-1})			High PPFD (750 µmol m^{-2}•s^{-1})		
	20 °C	24 °C	28 °C	20 °C	24 °C	28 °C	20 °C	24 °C	28 °C
RMSE, g_{FW}·$plant^{-1}$	2.1	8.8	6.6	12.2	12.3	18.2	16.2	16.0	14.5
CVRMSE, %	2.3	10.1	6.3	13.9	18.1	18.7	10.6	18.2	17.2
MAD, g_{FW}·$plant^{-1}$	2.9	15.9	14.1	19.2	19.9	35.2	17.9	31.3	26.4

Table 7
Relative differences for the specific energy demand, specific energy use and cultivation cycle using the growth models (initial & adjusted) compared to the results derived from an experimental growth dataset (Carotti et al., 2021).

Conditions		Relative difference, %							
		Dehumidification specific energy demand		Heating specific energy demand		Specific energy use		Cultivation cycle	
		Initial	Adjusted	Initial	Adjusted	Initial	Adjusted	Initial	Adjusted
Low	20 °C	49.3	0.5	60.4	1.4	18.2	1.0	24.0	1.2
PPFD	24 °C	40.7	0.3	47.8	1.3	4.9	0.9	14.9	3.1
	28 °C	65.4	2.5	66.8	4.1	5.3	0.5	16.2	1.7
Medium	20 °C	49.8	0.0	68.3	1.7	8.4	1.6	12.8	3.5
PPFD	24 °C	77.7	5.2	91.3	0.0	8.7	3.5	2.2	0.7
	28 °C	79.4	0.1	122.3	8.0	3.5	1.5	18.0	3.4
High	20 °C	24.5	0.0	57.1	3.2	15.9	1.2	14.9	0.2
PPFD	24 °C	38.3	0.0	83.3	2.6	14.3	2.4	17.7	4.1
	28 °C	76.5	2.0	153.5	10.4	22.0	0.1	28.2	1.2

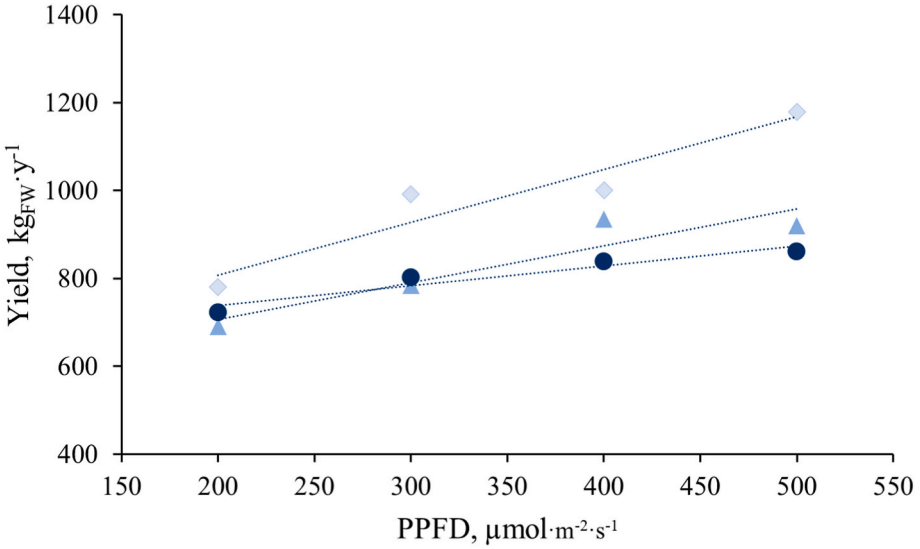

Fig. 9. Estimated yield with the adjusted growth model for different lighting intensity for ▲ 20 °C, ◇ 24 °C, and ● 28 °C.

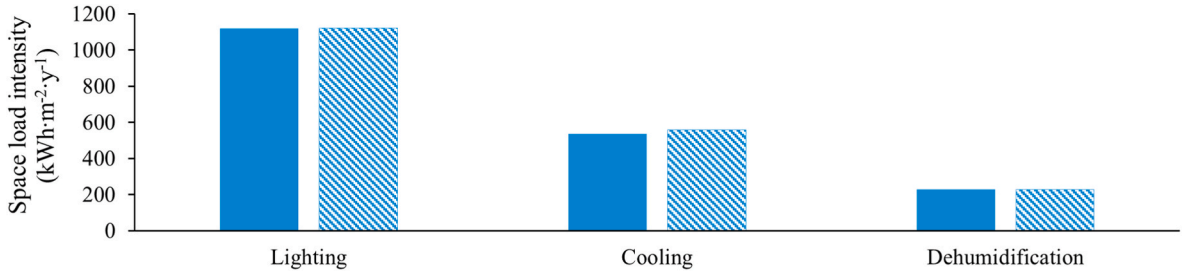

Fig. 10. Comparison of the energy use intensity estimated by Graamans et al. (2018) (solid bars) and the ones from the current study as a verification step (hatched bars).

confirming the proper implementation of the energy modelling approach.

4. Discussion

The results obtained from this study are not easily comparable to data available in the literature since the specific energy use is rarely reported, unlike the specific energy consumption, which is based on the consumption of the HVAC equipment and lighting. Since several parameters influence the HVAC equipment design and performance, estimating their energy consumption adds a layer of complexity for comparative analyses. For example, Weidner, Yang, and Hamm (2021) compared the specific energy consumption of various high-density CEA spaces modelled reported in the literature. The authors noted a significant disparity in specific energy consumption, ranging from approximately 3.2 to 59.1 $kWh \cdot kg_{FW}^{-1}$, which can be partially explained by important differences regarding the HVAC equipment design and performances. The disparity can also be attributed to differences in maintained indoor environment conditions, cultivation methods, location, envelope characteristics and energy modelling approach.

Graamans et al. (2018) are some of the few researchers who have reported specific energy use. Their model estimated yield using the growth model developed by Van Henten (1994) with specific energy use ranging from 1420 to 1489 $MJ \cdot kg_{DW}^{-1}$, depending on the location. This corresponds to a specific energy use of 15.5–15.6 $kWh \cdot kg_{FW}^{-1}$ for a dry matter content of 3.9%, which aligns with the results shown in Fig. 6. However, it is important to highlight that this comparison has limitations mainly due to (1) disparities in the modelling parameters, such as the indoor environment conditions and possibly the weight of crops at transplant and harvest, and (2) the modelling approach. The main distinction in indoor environment conditions is the use of floating setpoints for indoor air temperature and relative humidity rather than tightly controlling them to a fixed value. As for the modelling approach, Graamans et al. (2018) did not use a growth model to estimate crops heat gain/loss; the LAI was set to a constant value over the simulation period. As specified in section 3.4, the impact of light interception on lighting heat gain was also neglected, and moisture removal associated with the sensible cooling process was included. When the latter (moisture removal) is factored into estimating the energy demand, it allows for the direct sizing of the dehumidification system based on the dehumidification energy demand. Conversely, omitting moisture removal might necessitate an intermediary step to size the dehumidification system using the dehumidification energy demand. However, this approach provides a comprehensive understanding of the space energy requirements for the proper sizing of the HVAC system since it supports calculating the space sensible heat ratio (SHR). As an example of the usefulness of this approach, it becomes apparent that towards the end of the cultivation cycle, the dehumidification energy demand increases, leading to a reduction of the SHR of the space. Consequently, selecting a cooling system that can deliver a low SHR would be better since it would be most efficient. Another example is if a heat recovery loop is used to cool LED lights. This type of cooling system does not contribute to any moisture removal from the air. As such, moisture removal associated with the sensible cooling process should not be included in the energy modelling approach.

It is important to underline some of the limitations of the developed crop model. One key parameter in the growth model, the dry matter content, has a significant influence over two main outputs: yield and heat gain/loss from crops. In the developed growth model, the dry weight is first estimated to subsequently derive the fresh weight and the LAI using the dry matter content. However, in comparison to data available in the literature, the dry matter contents used in this study (2.6, 3.8 and 4.2%, as specified in Table 3) are lower than those reported by Meinen, Dueck, Kempkes, and Stanghellini (2018), which ranged from 5.8% to 8.4% for the same variety (‘*Othilie*’). Thus, the results obtained in this study, such as the specific energy demand and specific energy use, could be limited to ‘*Othilie*’ lettuces with relatively low dry matter content.

Furthermore, the developed growth model exhibits additional limitations, such as being tailored for a harvest weight equal to or smaller than $250 g_{FW}$ per plant, constrained to well-irrigated crops with adequate nutrients, specific to the indoor conditions that fall into the range of the experimental dataset used and specific to ‘*Othilie*’ variety cultivated by Carotti et al. (2021). To perform energy analysis with indoor conditions that do not fall into the range of the experimental dataset used and/or other variety of lettuces, the sensible parameters could be calibrated using the approach proposed in this study for another experimental growth dataset and specific model parameters, such as the SLA and the dry matter content, should be adjusted.

The developed crop model is tailored for high-density CEA applications and is part of a versatile approach. The model was developed to model spaces with solar and/or electric lighting for various planting crop densities and photoperiods. Dynamic moisture air properties also included in the model to support future calibrations under less common indoor air conditions. The next step would entail applying the same approach used in this study to other CEA applications, such as a closed greenhouse with electric lighting. This would require verifying and adjusting the growth model, if necessary. Additionally, the methodology developed in this study could potentially be applied to adapt the crop model to other leafy greens, such as kale and spinach.

5. Conclusion

In this paper, a grey-box growth model was developed to estimate the yield, the energy demand and the energy use of high-density controlled environment agriculture (CEA) spaces. The model builds upon an existing lettuce growth model, initially developed for greenhouses by Van Henten (1994) and adjusted by modifying specific parameters and calibrating the most sensitive ones. The calibrations were completed using an experimental growth dataset containing nine sets of indoor environment conditions for lettuce grown in a high-density CEA space. Two indicators were used to assess the model performance: specific energy demand and specific energy use. Before the proposed modifications and calibration, the initial model overestimated the leaf area index, which led to higher specific energy demand for heating and dehumidification. It also overestimated the growth rate, leading to underestimating the specific energy use for most conditions.

This initial assessment highlighted that the model must be adjusted for controlled environment agriculture applications. Specific parameters were thus modified according to available values in the literature and better suited to high-density CEA applications, and four sensitive parameters were calibrated. The model calibration was completed over the shoot fresh weight using a genetic algorithm with an objective function that minimised the root mean square error. This resulted in a parametrisation of four sensitive parameters (c_ε, c_β, k_s, $c_{gr,max}$), using nine sets of conditions. The dynamic crop model was developed as a grey-box model, incorporating the heat exchanges of crops as they grow to a high-density CEA space modelled in the TRNSYS software. Moreover, the dynamic crop model can be used for energy analysis of indoor environment conditions that fall within the range of conditions used in this study by interpolating the sensitive parameters. The calibration approach could be used to parametrise the model for other cultivars and indoor conditions.

This contribution allows, through a transient approach, the estimation of yield, energy demand and energy use considering crop growth for a wide range of indoor environment conditions commonly selected to grow lettuce in CEA spaces. These are essential to complete energy, financial and environmental analyses and to support optimisation of the trade-off between crop growth and energy requirements.

Data availability

The dynamic crop model developed in this paper is available as a TRNSYS component on GitHub. For access, consult the GitHub page of the Laboratory of Thermal and Building Science of ETS Montreal.

Declaration of generative AI and AI-assisted technologies in the writing process

While preparing this work, the authors used ChatGPT (GPT-3.5) to improve the language and readability of a few sentences (less than 10% of the text). After using this tool/service, the authors reviewed and edited the content as needed and took full responsibility for the content of the publication.

Declaration of competing interest

The authors declare that they have no known competing financial interests or personal relationships that could have appeared to influence the work reported in this paper.

Acknowledgments

This work was supported by the Fonds de recherche du Québec – Nature et technologies (Quebec, Canada), PhD scholarship for the first co-author, as well as NSERC research grants RGPIN-2020-04576 and ALLRP 561361-21.

Appendix A. Supplementary data

Supplementary data to this article can be found online at https://doi.org/10.1016/j.biosystemseng.2023.12.012.

References

Architecture, & WayBeyond. (2021). *Global CEA census report*.

Baba, F. M., Ge, H., Zmeureanu, R., & Wang, L. (2022). Calibration of building model based on indoor temperature for overheating assessment using genetic algorithm: Methodology, evaluation criteria, and case study. *Building and Environment, 207*, Article 108518. https://doi.org/10.1016/j.buildenv.2021.108518

Baglivo, C., Mazzeo, D., Panico, S., Bonuso, S., Matera, N., Congedo, P. M., et al. (2020). Complete greenhouse dynamic simulation tool to assess the crop thermal well-being and energy needs. *Applied Thermal Engineering, 179*, Article 115698. https://doi.org/10.1016/j.applthermaleng.2020.115698

Benis, K., Reinhart, C., & Ferrão, P. (2017). Development of a simulation-based decision support workflow for the implementation of Building-Integrated Agriculture (BIA) in urban contexts. *Journal of Cleaner Production, 147*, 589–602. https://doi.org/10.1016/j.jclepro.2017.01.130

Both, A.-J. (1995). *Dynamic simulation of supplemental lighting for greenhouse hydroponic lettuce production*. Ann Arbor: Ph.D., Cornell University.

Carotti, L., Graamans, L., Puksic, F., Butturini, M., Meinen, E., Heuvelink, E., et al. (2021). Plant factories are heating up: Hunting for the best combination of light intensity, air temperature and root-zone temperature in lettuce production. *Frontiers in Plant Science, 11*. https://doi.org/10.3389/fpls.2020.592171, 592171-592171.

Chang, C.-L., Chung, S.-C., Fu, W.-L., & Huang, C.-C. (2021). Artificial intelligence approaches to predict growth, harvest day, and quality of lettuce (Lactuca sativa L.) in a IoT-enabled greenhouse system. *Biosystems Engineering, 212*, 77–105. https://doi.org/10.1016/j.biosystemseng.2021.09.015

Coakley, D., Raftery, P., & Keane, M. (2014). A review of methods to match building energy simulation models to measured data. *Renewable and Sustainable Energy Reviews, 37*, 123–141. https://doi.org/10.1016/j.rser.2014.05.007

Cohen, A. R., Chen, G., Berger, E. M., Warrier, S., Lan, G., Grubert, E., et al. (2022). Dynamically controlled environment agriculture: Integrating machine learning and mechanistic and physiological models for sustainable food cultivation. *ACS ES&T Engineering, 2*(1), 3–19. https://doi.org/10.1021/acsestengg.1c00269

Critten, D. (1991). Optimization of CO2 concentration in greenhouses: A modelling analysis for the lettuce crop. *Journal of Agricultural Engineering Research, 48*, 261–271.

Dorais, M. (2003). The use of supplemental lighting for vegetable crop production: Light intensity, crop response, nutrition, crop management, cultural practices. In *Canadian greenhouse conference* (pp. 1–8). Toronto: Canada.

El Ghoumari, M. Y., Tantau, H. J., & Serrano, J. (2005). Non-linear constrained MPC: Real-time implementation of greenhouse air temperature control. *Computers and Electronics in Agriculture, 49*(3), 345–356. https://doi.org/10.1016/j.compag.2005.08.005

Fraile-Robayo, R. D., Álvarez-Herrera, J. G., Reyes, M., A, J., Álvarez-Herrera, O. F., & Fraile-Robayo, A. L. (2017). Evaluation of the growth and quality of lettuce (*Lactuca sativa* L.) in a closed recirculating hydroponic system. *Agronomía Colombiana, 35*, 216–222. https://doi.org/10.15446/agron.colomb.v35n2.63439

Graamans, L., Baeza, E., van den Dobbelsteen, A., Tsafaras, I., & Stanghellini, C. (2018). Plant factories versus greenhouses: Comparison of resource use efficiency. *Agricultural Systems, 160*(Supplement C), 31–43. https://doi.org/10.1016/j.agsy.2017.11.003

Graamans, L., van den Dobbelsteen, A., Meinen, E., & Stanghellini, C. (2017). Plant factories; crop transpiration and energy balance. *Agricultural Systems, 153* (Supplement C), 138–147. https://doi.org/10.1016/j.agsy.2017.01.003

Hang, T., Lu, N., Takagaki, M., & Mao, H. (2019). Leaf area model based on thermal effectiveness and photosynthetically active radiation in lettuce grown in mini-plant factories under different light cycles. *Scientia Horticulturae, 252*, 113–120. https://doi.org/10.1016/j.scienta.2019.03.057

Harbick, K., & Albright, L. (2016). Comparison of energy consumption: Greenhouses and plant factories. *VIII International Symposium on Light in Horticulture, 1134*, 285–292.

Iddio, E., Wang, L., Thomas, Y., McMorrow, G., & Denzer, A. (2020). Energy efficient operation and modeling for greenhouses: A literature review. *Renewable and Sustainable Energy Reviews, 117*, Article 109480. https://doi.org/10.1016/j.rser.2019.109480

Jans-Singh, M., Ward, R., & Choudhary, R. (2021). Co-simulating a greenhouse in a building to quantify co-benefits of different coupled configurations. *Journal of Building Performance Simulation, 14*(3), 247–276. https://doi.org/10.1080/19401493.2021.1908426

Jin, W., Formiga Lopez, D., Heuvelink, E., & Marcelis, L. F. M. (2023). Light use efficiency of lettuce cultivation in vertical farms compared with greenhouse and field. *Food and Energy Security, 12*(1), Article e391. https://doi.org/10.1002/fes3.39

Katsoulas, N., & Stanghellini, C. (2019). Modelling crop transpiration in greenhouses: Different models for different applications. *Agronomy, 9*, 392. https://doi.org/10.3390/agronomy9070392

Klein, S. A., & al, e. (2017). *Trnsys 18: A transient system simulation program*. Madison, WI, USA: Solar Energy Laboratory, University of Wisconsin.

Kokogiannakis, G., & Cooper, P. (2015). Evaluating the environmental performance of indoor plants in buildings. In *14th international conference of IBPSA - building simulation 2015, BS 2015, conference proceedings* (pp. 712–719).

Kozai, T. (2016). Why LED lighting for urban agriculture?. In *LED lighting for urban agriculture* (pp. 3–18). Springer.

Lalonde, T., Talbot, M. H., & Monfet, D. (2019). The impact of plants on HVAC system performance. In *Cold climate: A parametric study presented at building simulation 2019*. Montreal.

Ledesma, G., Nikolic, J., & Pons-Valladares, O. (2022). Co-simulation for thermodynamic coupling of crops in buildings. Case study of free-running schools in Quito, Ecuador. *Building and Environment, 207*, Article 108407. https://doi.org/10.1016/j.buildenv.2021.108407

Liebman-Pelaez, M., Kongoletos, J., Norford, L. K., & Reinhart, C. (2021). Validation of a building energy model of a hydroponic container farm and its application in urban design. *Energy and Buildings, 250*, Article 111192. https://doi.org/10.1016/j.enbuild.2021.111192

López-Cruz, I. L., Ruiz-García, A., Fitz-Rodríguez, E., Salazar-Moreno, R., & Rojano-Aguilar, A. (2017). A comparison of Bayesian and classical methods for parameter estimation in greenhouse crop models. *Acta Horticulturae, 1182*, 241–248. https://doi.org/10.17660/ActaHortic.2017.1182.29

Meinen, E., Dueck, T., Kempkes, F., & Stanghellini, C. (2018). Growing fresh food on future space missions: Environmental conditions and crop management. *Scientia Horticulturae, 235*, 270–278. https://doi.org/10.1016/j.scienta.2018.03.002

Nadal, A., Llorach-Massana, P., Cuerva, E., López-Capel, E., Montero, J. I., Josa, A., … Royapoor, M. (2017). Building-integrated rooftop greenhouses: An energy and environmental assessment in the mediterranean context. *Applied Energy, 187*, 338–351. https://doi.org/10.1016/j.apenergy.2016.11.051

Pearson, S., Wheeler, T. R., Hadley, P., & Wheldon, A. E. (1997). A validated model to predict the effects of environment on the growth of lettuce (Lactuca sativa L.): Implications for climate change. *Journal of Horticultural Science, 72*, 503–517. https://doi.org/10.1080/14620316.1997.11515538

Puccinelli, M., Malorgio, F., Pintimalli, L., Rosellini, I., & Pezzarossa, B. (2022). Biofortification of lettuce and basil seedlings to produce selenium enriched leafy vegetables. *Horticulturae, 8*(9), 801. https://doi.org/10.3390/horticulturae8090801

Ramirez, A., Rodriguez, F., Berenguel, M., & Heuvelink, E. (2003). Calibration and validation of complex and simplified tomato growth models for control purposes in the southeast of Spain. In *International workshop on models for plant growth and control of product quality in horticultural production* (Vol. 654, pp. 147–154).

Seginer, I., Straten, G., & Buwalda, F. (1998). Nitrate concentration in greenhouse lettuce : A modeling study. *Acta Horticulturae, 456*, 189–197. https://doi.org/10.17660/actahortic.1998.456.21

Shimizu, H., Kushida, M., & Fujinuma, W. (2008). A growth model for leaf lettuce under greenhouse environments. *Environment Control in Biology, 46*(4), 211–219.

Song, R., Liu, D., Pan, Y., Cheng, Y., & Meng, C. (2023). Container farms: Energy modeling considering crop growth and energy-saving potential in different climates. *Journal of Cleaner Production.* , Article 138353. https://doi.org/10.1016/j.jclepro.2023.138353

Stanghellini, C. (1987). *Transpiration of greenhouse crops. An aid to climate management*. PhD Thesis. Wageningen: Agricultural University.

Sweeney, D., Hand, D. W., Slack, G., & Thornley, J. H. M. (1981). Modelling the growth of winter lettuce. *Math. Plant Physiol.*, 217–229.

Talbot, M. H., Lalonde, T., Beaulac, A., Haillot, D., & Monfet, D. (2022). Comparing the energy performance of different controlled environment agriculture spaces using TRNSYS. In *Proceedings of eSim 2022: 12th conference of IBPSA-Canada*.

Talbot, M.-H., & Monfet, D. (2020). Estimating the impact of crops on peak loads of a Building-Integrated Agriculture space. *Science and Technology for the Built Environment, 26*(10), 1448–1460. https://doi.org/10.1080/23744731.2020.1806594

Talbot, M. H., & Monfet, D. (2021). Estimated energy demand and sensible heat ratio of a controlled-environment agriculture space for a growth cycle. *ASHRAE Transactions, 127*(2), 211–219.

Tei, F., Scaife, A., & Aikman, D. P. (1996). Growth of lettuce, onion, and red beet. 1. Growth analysis, light interception, and radiation use efficiency. *Annals of Botany, 78*(5), 633–643. https://doi.org/10.1006/anbo.1996.0171

Van Henten, E. J. (1994). Validation of a dynamic lettuce growth model for greenhouse climate control. *Agricultural Systems, 45*(1), 55–72. https://doi.org/10.1016/S0308-521X(94)90280-1

Van Henten, E. J., & Van Straten, G. (1994). Sensitivity analysis of a dynamic growth model of lettuce. *Journal of Agricultural Engineering Research, 59*(1), 19–31. https://doi.org/10.1006/jaer.1994.1061

Vanthoor, B. H. E., de Visser, P. H. B., Stanghellini, C., & van Henten, E. J. (2011). A methodology for model-based greenhouse design: Part 2, description and validation of a tomato yield model. *Biosystems Engineering, 110*(4), 378–395. https://doi.org/10.1016/j.biosystemseng.2011.08.005

Ward, R., Choudhary, R., Cundy, C., Johnson, G., & McRobie, A. (2015). Simulation of plants in buildings; incorporating plant-Air interactions in building energy simulation. In *14th conference of international building performance simulation association*. International Building Performance Simulation Association. BS 2015, December 7, 2015 - December 9, 2015.

Watson, D. J. (1947). Comparative physiological studies on the growth of field crops: I. Variation in net assimilation rate and leaf area between species and varieties, and within and between years. *Annals of Botany, 11*(41), 41–76.

Weidner, T., Yang, A., & Hamm, M. W. (2021). Energy optimisation of plant factories and greenhouses for different climatic conditions. *Energy Conversion and Management, 243*, Article 114336. https://doi.org/10.1016/j.enconman.2021.114336

Yeo, U.-H., Lee, S.-Y., Park, S.-J., Kim, J.-G., Choi, Y.-B., Kim, R.-W., … Lee, I.-B. (2022). Rooftop greenhouse: (1) design and validation of a BES model for a plastic-covered greenhouse considering the tomato crop model and natural ventilation characteristics. *Agriculture, 12*(7), 903. https://doi.org/10.3390/agriculture12070903

Zhang, K., Burns, I. G., & Turner, M. K. (2008). Derivation of a dynamic model of the kinetics of nitrogen uptake throughout the growth of lettuce: Calibration and validation. *Journal of Plant Nutrition, 31*(8), 1440–1460. https://doi.org/10.1080/01904160802208345

Zhang, Y., & Kacira, M. (2020). Enhancing resource use efficiency in plant factory. *Acta Horticulturae, 1271*, 307–314. https://doi.org/10.17660/ActaHortic.2020.1271.42